IOP Publishing Journal Title
Journal **XX** (XXXX) XXXXXX https://doi.org/XXXX/XXXX

Measuring the air fraction and the gas temperature in non-thermal argon plasma jets through the study of the air influence on the collisional broadening of some argon atomic emission lines

Maria C. Garcia[1], Cristina Yubero[2], and Antonio Rodero[2]

[1] Department of Applied Physics, C-2 Building, University of Cordoba, 14071 Cordoba, Spain
[2] Department of Physics, C-2 Building, University of Cordoba, 14071 Cordoba, Spain

E-mail: fa1gamam@uco.es

Received xxxxxx
Accepted for publication xxxxxx
Published xxxxxx

Abstract

Cold atmospheric argon plasma jets have shown to be very promising in medicine and they are being currently used for therapeutical uses as the healing of wounds or the treatment of tumors. Because they run in the open atmosphere, they generate copious amounts of reactive oxygen and nitrogen species, which play an outstanding role in their biological action. But, in this kind of reactors, unknown amounts of air enter the plasma region depending on the experimental conditions, changing the chemistry in them, and eventually their effects. In this work, we propose a new spectroscopic method to measure the amount of air in argon non-thermal (including cold atmospheric) plasma jets through the collisional broadening of Ar I 840.86 and Ar I 842.46 nm emission lines. The method allows the simultaneous determination of the gas temperature. For validation purposes, it was applied to a microwave-induced plasma jet working at different operational conditions. Results were consistent with those obtained from the rotational temperature derived from simulations of N_2 (2^{nd} positive system) rovibrational band.

Keywords: atmospheric pressure plasma, cold atmospheric plasma, plasma diagnosis, emission spectroscopy, gas temperature

1. Introduction

In the last twenty years, the development of non-thermal plasma sources well-controlled and open to the atmosphere, generating *cold atmospheric plasmas* (CAPs) at temperatures under 40 ºC, has proliferated opening new horizons in fields such as biomedicine, food preservation, and agriculture [1-3]. CAPs emerge as a very appealing technology because of their easy handling (they run at atmospheric pressure, so without the restrictions imposed by vacuum systems), their low power consumption, along with their ability to generate active species, in great quantity and diversity. Controlling the gas temperature (T_g) of CAPs is particularly relevant when it comes to applying cold plasma jets directly on living human

(and animal) cells, tissues and organs, and in the treatment of foods and plants.

Since CAP sources run open to the atmosphere, there is an interaction plasma-air, which eventually results in the generation of abundant amounts of reactive oxygen and nitrogen species, also known as ROS and RNS respectively (more generally RONS). Recent studies have shown that RONS play an outstanding role in the biological action of CAPs [4-12]. Thus, knowing all species generated in CAPs is one main step to understand, control, and manage their biological effects.

The development of new diagnosis techniques allowing both the identification of species created in CAPs (and their concentrations) and obtaining reliable values of the gas temperature is of great interest, along with the development of models aiming at understanding the plasma-tissue (food/plant) interaction.

Argon is commonly used in the operation of CAPs reactors because it is a cheap inert gas. Some of these reactors, such as PlasmaDerm, kiNPEn, or MicroPlaSter, have even been marketed as therapeutic tools. As they are generated in the open atmosphere, unknown amounts of air (dependent on the experimental conditions) enter the plasma region. To have an estimation of the proportion of air in these discharges is of paramount importance from the perspective of their modeling. Also, it would help to understand experimental results dealing with the behavior and effectiveness of the different plasma sources determined by the amount and variety of species in them.

The gas temperature in atmospheric-pressure plasmas is frequently determined from UV-Optical Emission Spectroscopy (UV-OES) techniques based on the analysis of molecular emission spectra. Under such a high-pressure condition, translational and rotational energy states are strongly coupled, and the rotational temperature resulting from them is a good estimate of the kinetic temperature of the plasma heavy particles (ions and neutrals). However, the application of molecular emission spectroscopy techniques for gas temperature determination in plasmas is sometimes complex and should be done carefully [13]. Thus, for instance, an overlap of bands or a population distribution of rotational levels with a non-Boltzmann nature prevents getting reliable values of gas temperature. Besides, some of these techniques are not sensitive to variations of the gas temperature near the room temperature (so, under CAP conditions) [14].

More recently, they have been developed alternative OES methods allowing the gas temperature determination in non-thermal plasmas, based on the analysis of profiles of some specific atomic lines. The main feature of these methods is they do not rely on thermodynamic equilibrium assumptions. Christova and colleagues proposed, for the first time, the use of the *van der Waals* broadening of some argon atomic lines for the determination of the plasma gas temperature [15]. Briefly, this technique, further developed in [16,17], consists in the measurement of argon atomic lines not experiencing resonance broadening (also dependent on T_g), namely Ar I 425.94, 522.13, 549.61 and 603.21 nm. Because, these lines have a non-negligible *Stark* broadening (dependent on electron density) for electron densities above 10^{14} cm^{-3}, this technique requires previous determination of this plasma parameter. Yubero and colleagues proposed an approach using pairs of these lines in order to bypass this dependence on the electron density [18].

Pipa and colleagues [14] developed a method based on the measurement of the *resonance* broadening Ar I 750.39, 826.45, 840.82, 852.14, 922.45, and 978.45 nm emission lines. These lines correspond to transitions into the resonance level s_2 of the $3p^5 4s$ configuration. For electron densities lower than 10^{15} cm^{-3}, these lines have a negligible Stark broadening. They also considered negligible the van der Waals broadening of these lines.

More recently, we analysed in detail the relative importance of resonance and van der Waals broadenings of all argon atomic lines corresponding to transitions into resonance levels *s2* and *s4* of the *3p54s* configuration [19]. In that work, we demonstrated for these lines the van der Waals contribution to the entire broadening should be considered under any gas temperature condition. We also proposed new methods to measure the gas temperature in pure argon plasmas from the collisional broadening of any of these lines. When these methods were applied to a plasma jet, results from them showed some discrepancies for plasma positions in contact with air, which were minimized considering a typical proportion of air in calculations.

On the basis that van der Waals and resonance contributions depend on the composition of the gas supporting the discharge, in a specific way for each of the argon lines in reference [19] (as it will be shown in next section), in the present work we propose a new approach based on the use of two of these lines, enabling simultaneous determination of gas temperature and amount of air in non-thermal argon plasma jets with gas temperatures below 2000 K and electron densities under 10^{15} cm^{-3} (so, including argon CAPs). For non-thermal plasma jets operating in other gases, similar methods using different atomic lines (He I, O I…) could be also developed. In contrast to other OES techniques, this new method has the additional advantage of no relying on thermodynamic equilibrium assumptions and not being affected by spatial non-uniformities as these broadenings are determined by local particle collisions.

The method has been applied to the case of an argon microwave-induced plasma jet (2.45 GHz). For validation purposes, a comparison of T_{gas} to the rotational temperature, derived after the N_2 rovibrational band simulations, was done.To the best of the author's knowledge, this is the first

time that OES is being used to evaluate the fraction of air in a plasma.

2. Method

In plasmas generated at atmospheric pressure, the emission of atoms broads due to different effects. For a detailed description of these broadening mechanisms, the reader is referred to references [13,14,17,20].

Briefly, lines emitted by an unmagnetized plasma are generally affected by (i) the *natural broadening*; (ii) the *Doppler broadening*; and (iii) the *collisional broadening*. Emission from the plasma could be partially self-absorbed as it propagates within it. This self-absorption phenomenon artificially modifies the broadening of lines and is difficult to quantify. For this reason, atomic lines non-affected by self-absorption are preferably used for plasma diagnosis. Finally, when lines are detected by the optical system, they also experience an *instrumental broadening*, determined by the dispersion and the width of the slits when a spectrometer is used for the detection of light [20].

Because the *natural broadening* is typically in the order of 0.00001 nm, it is neglected in atmospheric pressure plasma spectroscopy.

The *Doppler broadening* originates a Gaussian-shaped line profile with a full-width at half-maximum (FWHM), W_D, dependent on the line wavelength (λ), the gas temperature in the plasma and the mass of the radiating atoms [20].

The *collisional broadening* encompasses *van der Waals*, *resonance*, and *Stark* broadenings originated by disturbing particles of different nature. The *van der Waals* broadening is due to neutral perturbers and originates line profiles with a Lorentzian shape, whose FWHM (W_W) is determined by T_g and it is also dependent on λ, the nature of the emitter atoms, and the nature of perturbers, all gathered in C_W constant [19]

$$W_W(T_g) = \frac{C_W}{T_g^{0.7}}(\text{nm}) \tag{1}$$

The value of this constant for a specific Ar I line can be calculated using expressions in [19] and taking into account the considerations below. In a pure argon plasma, argon atoms would be the only perturbers surrounding emitters, so reduced mass Ar-Ar ($\mu_{Ar\text{-}Ar}$ = 19.97) and argon polarizability (α_{Ar} = $16.54\cdot10^{-25}$ cm^3) must be used for the determination of C_W^{Ar}. In argon plasmas containing air, air molecules should be also considered as perturbers and in that case, reduced mass Ar-Air ($\mu_{Ar\text{-}Air} \approx 16.81$) and air polarizability ($\alpha_{Air} \approx 2.10\cdot10^{-23}$ cm^3) need be considered to determine C_W^{Air}. In this way, for an argon jet (open to the air), the following expression of the van der Waals broadening would account for the air entrainment into the plasma [13]

$$W_W(T_g, \chi_{Air}) = \chi_{Ar}\frac{C_W^{Ar}}{T_g^{0.7}} + \chi_{Air}\frac{C_W^{Air}}{T_g^{0.7}}(\text{nm}) = \\ = (1-\chi_{Air})\frac{C_W^{Ar}}{T_g^{0.7}} + \chi_{Air}\frac{C_W^{Air}}{T_g^{0.7}}(\text{nm}) \tag{2}$$

being χ_{Ar} and χ_{Air} the molar fractions of argon and air, respectively [17].

On the other hand, dipole-dipole interactions of the emitter with ground-state atoms of the same element are responsible for the *resonance broadening*. This broadening leads to a Lorentzian shaped profile, whose FWHM (W_R) depends again on T_g and λ of the line, in addition to some spectroscopic parameters (oscillator strength, wavelength, the statistical weights of its upper and lower levels) of the so-called *resonance lines* involved in each case [19]. Again, all these dependencies can be gathered in a constant C_R in such a way that W_R can be written as

$$W_R(T_g) = \frac{C_R}{T_g}(nm) \tag{3}$$

Let's remind that this broadening is not affecting every single spectral line in the spectrum, but only those corresponding to transitions with upper and lower levels having electric dipole transitions to the ground state.

When a fraction of air is present in the discharge, the proportion of argon atoms in the ground state reduces, and the expression (3) should be modified as follows

$$W_R(T_g, \chi_{Air}) = \chi_{Ar}\frac{C_R}{T_g}(\text{nm}) = (1-\chi_{Air})\frac{C_R}{T_g}(\text{nm}) \tag{4}$$

The *Stark broadening* of the line is caused by charged particles around the emitter atom. In non-thermal plasmas, electrons are responsible for the foremost part of this broadening (due to their higher velocities compared with that of ions). For argon atoms (non-hydrogenic), the Stark broadening due to electrons results in a profile that can be approximated to a Lorentzian function, and whose FWHM, W_S, depends on the electron density (n_e) and the electron temperature (T_e) (through the so-called Stark parameter $w_e(T_e)$) as follows [21-24]:

$$W_S(T_e, n_e) \approx w_e(T_e)\frac{n_e}{10^{16}} \tag{5}$$

In summary, the collisional broadening (resulting from *van der Waals*, *resonance*, and *Stark* mechanisms) leads to a Lorentzian-shaped profile with an FWHM, W_C, given by:

$$W_C(T_g, \chi_{Air}, n_e, T_e) = W_W(T_g, \chi_{Air}) + W_R(T_g, \chi_{Air}) + W_S(n_e, T_e) \quad (6)$$

Using entrance and exit slits of equal width during detection with the spectrometer, the instrumental function can be approximated to a Gaussian profile with an FWHM, W_I, given by

$$W_I = D(\lambda) l_S \quad (7)$$

where l_s is the slit width and $D(\lambda)$ the dispersion of spectrometer, which depends on wavelength. For each line and given slit widths, this broadening can be determined.

Finally, the detected profile of a no self-absorbed line (resulting from the combination of Doppler, collisional and instrumental broadenings) can be reasonably well fitted in many cases to a Voigt function [15-20], whose FWHM (W_V), is given by:

$$W_V \approx \frac{W_C}{2} + \sqrt{\left(\frac{W_C}{2}\right)^2 + W_D^2 + W_I^2} \quad (8)$$

In this work, we propose a new tool allowing the simultaneous determination of T_g and the fraction of air in the plasma. The method is based on the measurement of the collisional broadening of two (non-self-absorbed) argon atomic lines, namely Ar I 840.86 and Ar I 842.46 nm. These lines correspond to transitions into the resonance levels s_2 and s_4, respectively, of the $3p^5 4s$ configuration, so they have a relatively large resonance broadening (particularly high in the case of the Ar I 840.86 nm line).

In previous work, we have shown that, for electron densities under 10^{15} cm^{-3}, resonance and van der Waals broadenings of both lines are much larger than their respective Stark broadenings [19], so that, the Stark contribution to the total collisional broadening can be neglected. Therefore, under these experimental conditions, W_C of these lines does not vary with n_e and T_e, being only dependent on T_g and χ_{Air}

$$W_C(T_g, \chi_{Air}) \approx W_W(T_g, \chi_{Air}) + W_R(T_g, \chi_{Air}) = (1-\chi_{Air})\frac{C_W^{Ar}}{T_g^{0.7}} + \chi_{Air}\frac{C_W^{Air}}{T_g^{0.7}} + (1-\chi_{Air})\frac{C_R}{T_g}\,(\text{nm}) \quad (9)$$

In this expression, an averaged effect of the air as perturber was considered [19], in the same way as proposed by Laux et al. in [25]. Bruggeman et al. [26] and Garcia et al. [27] did a similar assumption to determine the van der Waals contribution of the line H_β (hydrogen Balmer series) for plasmas in vapor water.

Given that constants C_W^{Ar}, C_W^{Air} and C_R in eq. (9) are characteristics to each specific line, using eq. (9) for two lines (in this case, Ar I 840.86 and Ar I 842.46 nm), T_g and the air fraction in plasma can be determined simultaneously.

Constants C_W^{Ar}, C_W^{Air} and C_R in eq. (9) have been calculated for Ar I 840.86 and Ar I 842.46 nm lines. Data from the NIST atomic database [28] and expressions in [19] were used for this purpose. In this way, the following values were obtained: C_W^{Ar}(Ar I 840.86 nm) = 2.100, C_W^{Air}(Ar I 840.86 nm) = 6.110, C_R(Ar I 840.86 nm) = 67.519, C_W^{Ar}(Ar I 842.46 nm) = 1.891, C_W^{Air}(Ar I 842.46 nm) = 5.502, C_R(Ar I 842.46 nm) = 16.802.

On the other hand, because of the Doppler broadening of the lines Ar I 840.86 and Ar I 842.46 nm only becomes important for values of gas temperature higher than 2000 K [19], eq. (8) can be written for plasmas with T_g < 2000 K as follows

$$W_V \approx \frac{W_C}{2} + \sqrt{\left(\frac{W_C}{2}\right)^2 + W_I^2} \quad (10)$$

Therefore, the whole procedure would be the following. Firstly, W_V would be obtained from the experimentally measured profile, by fitting it to Voigt shaped profile. Subsequently, knowing W_I, the collisional broadening would be derived from

$$W_C = W_V - \frac{W_I^2}{W_V} \quad (11)$$

Finally, using eq. (9) for Ar I 840.86 and Ar I 842.46 nm, unknowns T_g and χ_{Air} could be obtained.

As solving this system of equations is not straightforward, this technique has been simplified through the graphical method shown in Figure 1. This figure plots theoretical W_C (Ar I 842.46 nm) versus theoretical W_C (Ar I 840.86 nm) for different T_g and air molar fractions. It also includes a calculation example corresponding to a case in which W_C (Ar I 840.86) and W_C (Ar I 842.46) measured were 0.0808 and 0.0385 nm, respectively. In this example, the gas temperature and air fraction obtained were 900 K and 30%, respectively.

Let's remark that, as shown in Figure 1, the method becomes progressively more accurate as the gas temperature reduces and (in less extent) as the fraction of air does, so it is particularly adequate for CAPs.

Although in this work, the method has been developed for lines Ar I 840.86 and Ar I 842.46 nm (they are two of the most intense atomic argon lines and are isolated in the spectrum not

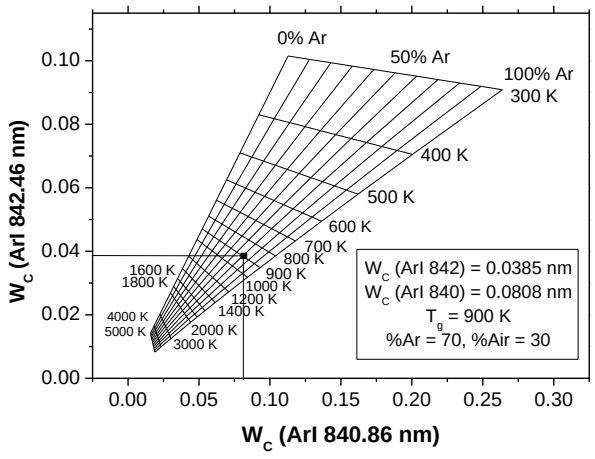

Figure 1. Theoretical dependence of W_C (Ar I 842.46 nm) and W_C (Ar I 840.86 nm) on T_g and air molar fractions.

overlapping with other peaks), other pairs of lines could be used as long as they fulfill the following conditions: (i) having a Stark broadening with a negligible contribution to the full collisional broadening (so a small value in comparison to resonance + van der Waals broadenings), (ii) undergoing negligible self-absorption and (iii) having broadenings with very different dependence on gas temperature and air amount, i.e. different C_R and C_W coefficients in Eq. 13. Pairs of argon lines corresponding to transitions into the resonance levels s_2 and s_4 of the $3p^5 4s$ configuration, respectively, satisfy these conditions.

3. Measuring the gas temperature and the air proportion in a microwave sustained plasma jet

3.1 Experimental set-up

The microwave (2.45 GHz) plasma jet was generated with the help of a *surfatron* [29] (see Figure 2) inside a quartz tube (of 1.5 and 4 mm of inner and outer diameter, respectively) opened to the air. This device launched azimuthally symmetric surface-waves, which mainly propagate through the dielectric-plasma interface, thus sustaining the plasma column inside the dielectric tube. In this way, microwave powers ranging from 30 to 200 W were coupled to the support gas (argon with a purity of ≥ 99.99 %). A calibrated mass flow controller was used for argon flow-rate adjustment at 0.5, 1.0 and 1.5 L/min. Figure 2 also schematizes the experimental acquisition system of UV-OES measurements. Light emission from the plasma axial position y = 18 mm (measuring y from the surfatron) was analyzed by using a 1 m focal length spectrometer (Jobin-Yvon THR1000, Czerny-Turner type), equipped with a 1200 grooves/mm holographic grating. A R636 Hamamatsu photomultiplier was used as a detector. The light from the plasma was transversely collected and focussed onto an optical fiber using an achromatic lens.

The instrumental function of the spectrometer for these wavelengths was measured following the procedure explained in reference [19]. For a 37 µm slit width, W_I (Ar I 840.82 nm) = 0.02827 nm and W_I (Ar I 842.46 nm) = 0.02829 nm.

On the other hand, in the chosen direction of observation (side-on), this plasma (of 1.5 mm max. diameter) can be considered optically thin for the lines Ar I 840.82 nm and 842.46 nm used in this work, as shown by Garcia *et al.* [30]. From light absorption measurements using an intense calibrated lamp, these authors measured a scape factor $\Lambda = 1$. In that study, lines with self-absorption were also identified because their populations deviated from the obtained Atomic State Distribution Function. Thus, lines Ar I 840.82 nm and 842.46 nm did not suffer self-absorption.

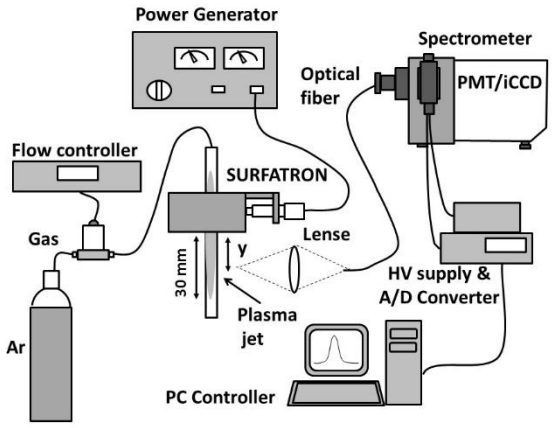

Figure 2. Experimental set-up.

In order to validate the gas temperature values measured, this magnitude was also estimated from the rotational temperature of the N_2 (C-B) rovibrational band (2^{nd} positive system). For this purpose, its emission at the region 350-360 nm was recorded and MassiveOES code developed by Voráč et al. [31] was used for the simulation the band at different rotational and vibrational temperatures. From the fitting of the simulated band to experimentally measured spectrum, the gas (rotational) temperature was estimated. Figure 3 illustrates an example of this fitting (for P = 150 W and F = 1 L/min).

Additionally, H I 486.13 nm line (Balmer series, H_β) was also recorded. Values of electron density derived from this line following the procedure described in [20], were lower than 10^{15} cm^{-3} (ranged between 1.4 and $4 \cdot 10^{14}$ cm^{-3}). So, based on previously explained considerations, the Stark mechanism broadening could be neglected.

The axial evolution of the emission of some atomic lines was also recorded. For this purpose, an iCCD (LAVISION Flamestar4) was used.

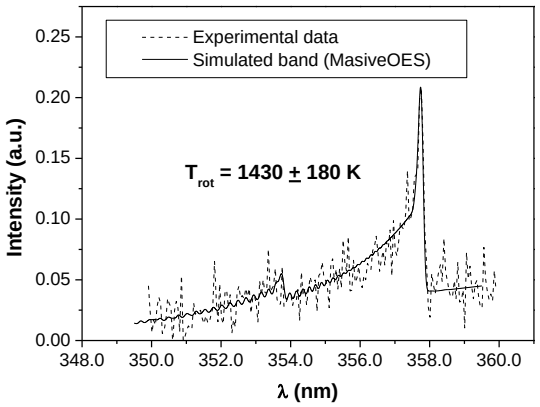

Figure 3. Fitting of experimenal N_2 rovibrational data to simulated N_2 rovibrational band by MasiveOES.

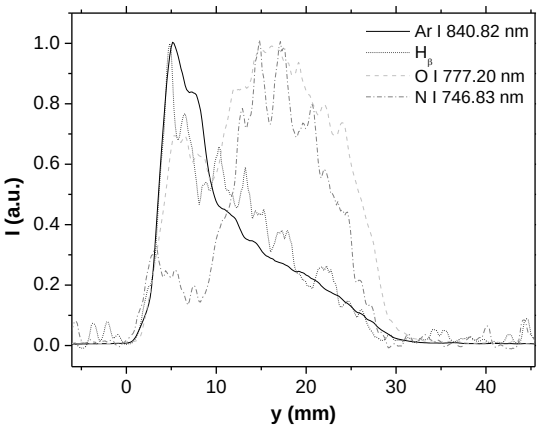

Figure 5. Axial changes for the intensities of the lines Ar I 840.82 nm, H_β, O I 777.20 nm, and N I 746.83 nm along the plasma jet (P = 150, F = 1 L/min).

3.2 Results

Figure 4 shows a typical emission spectrum recorded for this microwave plasma jet (P = 150 W, F = 1 L/min). The presence of N_2 bands and oxygen and nitrogen atomic lines reveals the air was indeed entering into the plasma. Axial changes for the intensities of the lines Ar I 840.82 nm, H_β, O I 777.20 nm, and N I 746.83 nm along the plasma jet in Figure 5 show that main excitation for nitrogen and oxygen atoms took place at positions closer the end of this plasma column with a maximum at $y \sim 18$ mm (when P = 150 W, F = 1 L/min). This indicates these species are reaching the plasma through the end of the tube. For this reason, measurements of air fraction and gas temperature were done at y = 18 mm. On the contrary, the highest excitation of argon and hydrogen (coming from the gas bottle) takes place at the positions next to the surfatron. For the rest of experimental conditions, measurents were also performed at this axial position.

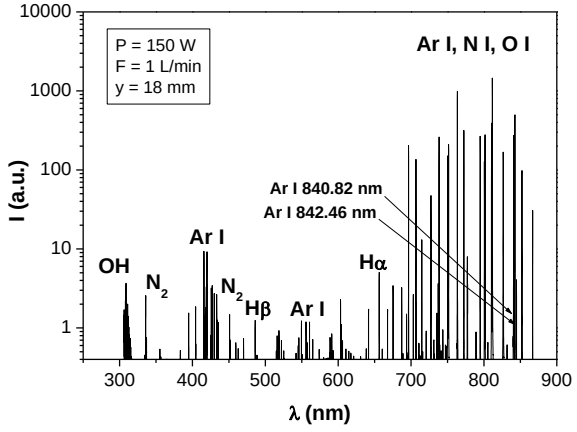

Figure 4. Characteristic emission spectrum emitted by the microwave argon plasma jet (P = 150 W, F = 1 L/min).

Table 1 gathers the collisional broadenings of the lines Ar I 840.82 nm and Ar I 842.46 nm emitted by the microwave plasma jet and measured under different operating conditions. From these values and using eq. (9) (or the plot in Figure 1), gas temperature and air fraction were obtained. Figure 6 shows the graphical determination of these parameters from the theoretical surface. Table 2 gathers results from it.

Table 1. Collisional broadening of Ar I 840.82 mn and Ar I 842.46 nm lines in a microvawe-sustained argon plasma jet running at different experimental conditions.

F_{Ar} (slm)	P(W)	$W_{C,\,840}$(nm)	$W_{C,\,842}$(nm)
0.5	30	0.0756 ± 0.0004	0.0325 ± 0.0004
	75	0.0632 ± 0.0004	0.0283 ± 0.0004
	150	0.0561 ± 0.0004	0.0262 ± 0.0003
	200	0.0507 ± 0.0005	0.0238 ± 0.0006
1.0	30	0.0816 ± 0.0004	0.0358 ± 0.0004
	75	0.0680 ± 0.0004	0.0307 ± 0.0004
	150	0.0556 ± 0.0006	0.0242 ± 0.0005
	200	0.0588 ± 0.0004	0.0276 ± 0.0003
1.5	30	0.0823 ± 0.0003	0.0380 ± 0.0004
	75	0.0703 ± 0.0003	0.0317 ± 0.0003
	150	0.0647 ± 0.0003	0.0321 ± 0.007
	200	0.0617 ± 0.0004	0.0290 ± 0.0003

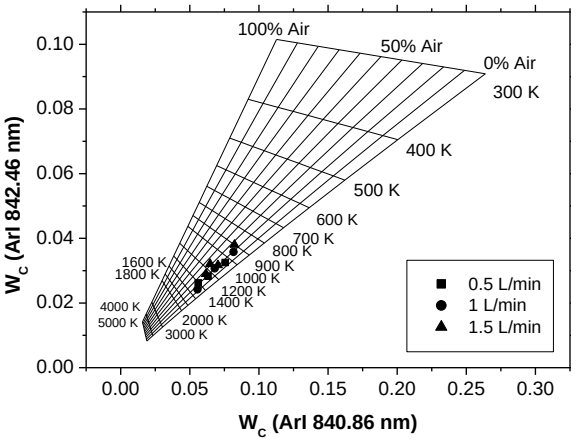

Figure 6. Graphical determination of gas temperature and air fraction in a microwave argon plasma jet under different experimental conditions.

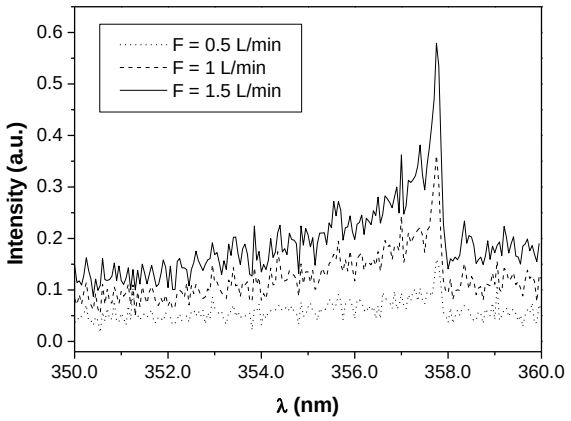

Figure 7. N_2 rovibrational bands measured at different gas flow-rates (P = 150 W, y = 18 mm).

Table 2. Gas temperature and air fraction in a microvawe argon plasma jet running at different experimental conditions.

F_{Ar} (L/min)	*P*(W)	T_g(K)	*% air*
0.5	30	1050 ± 30	15 ± 3
	75	1260 ± 30	18 ± 4
	150	1410 ± 20	22 ± 2
	200	1530 ± 40	13 ± 5
1.0	30	945 ± 15	19 ± 2
	75	1150 ± 20	20 ± 3
	150	1490 ± 40	12 ± 5
	200	1332 ± 15	23 ± 2
1.5	30	900 ± 10	26 ± 3
	75	1100 ± 10	19 ± 2
	150	1170 ± 40	28 ± 3
	200	1257 ± 15	24 ± 2

In general, in this plasma jet, the gas temperature grows when the power increases, under all flow rate conditions. On the contrary, the higher the flow rate, the lower the gas temperature. These results agree with others found in previous work [30].

The fraction of air in the plasma ranged between 12 ± 5 and 28 ± 3 %. For a fixed argon flow rate, this parameter has rather constant values, within the error range. Its mean values were 17%, 18.5%, and 24.5% for 0.5, 1.0 and 1.5 L/min, respectively. Thus, bigger amounts of air seem to be reaching the plasma at progressively higher argon flow rates. This increase is consistent with the rise in the emission of species coming from air observed at high flow-rates, and it is likely produced by the effect of turbulences at the exit of the tube under this high flow conditions. Figure 7 shows an example of this rise for N_2 (C) species at y = 18 mm.

The errors of the method in this plasma jet with gas temperatures above 1000 K are bigger than those expected for CAPs at temperatures under 320 K. A bigger plot of Figure 1, has been included as supplementary information as Figure S1, to be used by the reader.

On the other hand, Table 3 shows the values of gas temperature measured from the simulation of the N_2 band at the region 350-360 nm using MassiveOES. A good agreement was found.

Table 3. Gas temperature derived simulation of N_2 band at the region 350-360 nm.

F_{Ar} (L/min)	*P*(W)	$T_{g,\,N2}$ *(K)*
0.5	30	undetectable
	75	1160 ± 210
	150	1260 ± 190
	200	1410 ± 230
1.0	30	980 ± 240
	75	1130 ± 240
	150	1430 ± 180
	200	1400 ± 200
1.5	30	1100 ± 400
	75	1180 ± 160
	150	1130 ± 150
	200	1250 ± 140

4. Final remarks

In this work, we present a new spectroscopic method allowing the simultaneous determination of the gas temperature and air fraction in argon plasma jets in contact with air. It applies to non-thermal argon jets with gas temperatures under 2000 K and electron densities bellow 10^{15} cm^{-3}, which includes CAPs (as commercialized PlasmaDerm or kiNPEn). Nonetheless, the method could be properly modified to be applied to CAPs (or more gereally, to non-thermal plasmas with gas temperatures below 2000 K) operating with other noble gases as Helium.

In addition to having the interesting advantages related to OES techniques (easy to implement and not altering plasma properties), this method also provides the benefits of being very sensitive at low gas temperatures and no-based on thermodynamic equilibrium assumptions.

The new OES method proposed in this work was applied to an argon microwave jet open to the air. Values of the gas temperatures obtained from it were compared to the rotational temperatures derived from the N_2 rovibrational band and a very good agreement was found.

Acknowledgments

The authors thank the MINECO (project MAT2016-79866-R) for financial support.

References

[1] Woedtke T, Reuter S, Masur K, and Weltmann KD 2013 *Physics Reports* **530** 291
[2] Randeniya LK and Groot GJJB 2015 *Plasma Proces Polym* **12** 608
[3] Dasan BG, Onal-Ulusoy B, Pawlat J, Diatczyk J, Sen Y, and Mutlu M 2017 *Food Bioprocess Technol* **10** 650
[4] Graves DB 2012 *J Phys D: Appl Phys* **45** 263001
[5] Ahn HJ 2011 *PLoS ONE* **6** e28154
[6] Kaneko T, Sasaki S, Takashima K, and Kanzaki M 2017 *J Clin Biochem Nutr* **60** 3
[7] Tanaka H, Nakamura K, Mizuno M, Ishikawa K, Takeda K, Kajiyama H, Utsumi F, Kikkawa F, and Hori M 2016 *Scientific Reports* **6** 36282
[8] Canal C, Fontelo R, Hamouda I., Guillem-Marti J, Cvelbar U, and Ginebra MP 2017 *Free Radical Biology and Medicine* **110** 72
[9] Gümbel D, Bekeschus S, Gelbrich N, Napp M, Ekkernkamp A, Kramer A, and Stope MB 2017 *Int J Mol Sci* **18** 2004
[10] Liu Y, Tan S, Zhang H, Kong X, Ding L, Shen J, Lan Y, Cheng C, Zhu T, and Xia W 2017 *Scientific Reports* **7** 7980
[11] Sato Y, Yamada S, Takeda S, Hattori N, Nakamura K, Tanaka H, Mizuno M, Hori M, and Kodera Y 2018 *Ann Surg Oncol* **25** 299
[12] Szili EJ et al. 2018 *Plasma Sources Sci Technol* **27** 014001
[13] Yubero C, García MC, Varo M, and Martínez P 2013 *Spectrochimica Acta B* **90** 61
[14] Pipa AV, Ionikh Y, Chekishev VM, Dünnbier M and Reuter S 2015 *Appl Phys Lett* **106** 244104
[15] Christova M, Castaños-Martinez E, Calzada MD, Kabouzi Y, Luque JM, and Moisan M 2004 *Appl Spectrosc* **58** 1032
[16] Christova M, Gagov V and Koleva I 2000 *Spectrochim Acta B* **55** 815
[17] Yubero C, Dimitrijevic MS, García MC and Calzada MD 2007 *Spectrochim Acta B* **62** 169
[18] Yubero C, Rodero A, Dimitrijevic MS, Gamero A and García MC 2017 *Spectrochim Acta B* **129** 14
[19] Rodero A and García MC 2017 *J Quant Spectrosc & Radiat Transfer* **198** 93
[20] Nikiforov AY, Leys C, Gonzalez MA, Walsh JL 2015 *Plasma Sources Sci Technol* **24** 034001
[21] Konjevic N 1999 *Phys Rep* **316** 339
[22] Konjevic N and Wiese WL 1990 *J Phys Chem Ref Data* **19** 1307
[23] Konjevic N, Lesage A, Fuhr JR, and Wiese WL 2002 *J Phys Chem Ref Data* **31** 819
[24] Griem HR 1974 *Spectral line broadening by plasmas*, New York: Academic Press
[25] Laux CO, Spence TG, Kruger CH, and Zare RN 2003 *Plasma Sources Sci Technol* **12** 125
[26] Bruggeman P, Schram D, González MA, Rego R, Kong MG, and Leys C 2009 *Plasma Sources Sci Technol* **18** 025017
[27] García MC, Gucker SN and Foster JE 2015 *J Phys D: Appl Phys* **48** 355203
[28] Kramida A, Ralchenko Y and Reader J 2016 NIST ASD Team, NIST Atomic Spectra Database (version 5.7), available at http://physics.nist.gov/asd [Thu Jan 20, 2020]
[29] Moisan M and Pelletier J 1992 *Microwave excited plasmas* **Chap 3** Elsevier Amsterdam
[30] García MC, Rodero A, Sola A and Gamero A 2000 *Spectrochimica Acta B* **55** 1733
[31] Voráč J, Synek P, Potočňáková L, Hnilica J and Kudrle V 2017 *Plasma Sources Sci Technol* **2** 025010.

IOP Publishing Journal Title
Journal **XX** (XXXX) XXXXXX https://doi.org/XXXX/XXXX

Measuring the air fraction and the gas temperature in non-thermal argon plasma jets through the study of the air influence on the collisional broadening of some argon atomic emission lines

Maria C. Garcia[1], Cristina Yubero[2], and Antonio Rodero[2]

[1] Department of Applied Physics, C-2 Building, University of Cordoba, 14071 Cordoba, Spain
[2] Department of Physics, C-2 Building, University of Cordoba, 14071 Cordoba, Spain

E-mail: fa1gamam@uco.es

Received xxxxxx
Accepted for publication xxxxxx
Published xxxxxx

Abstract

Cold atmospheric argon plasma jets have shown to be very promising in medicine and they are being currently used for therapeutical uses as the healing of wounds or the treatment of tumors. Because they run in the open atmosphere, they generate copious amounts of reactive oxygen and nitrogen species, which play an outstanding role in their biological action. But, in this kind of reactors, unknown amounts of air enter the plasma region depending on the experimental conditions, changing the chemistry in them, and eventually their effects. In this work, we propose a new spectroscopic method to measure the amount of air in argon non-thermal (including cold atmospheric) plasma jets through the collisional broadening of Ar I 840.86 and Ar I 842.46 nm emission lines. The method allows the simultaneous determination of the gas temperature. For validation purposes, it was applied to a microwave-induced plasma jet working at different operational conditions. Results were consistent with those obtained from the rotational temperature derived from simulations of N_2 (2^{nd} positive system) rovibrational band.

Keywords: atmospheric pressure plasma, cold atmospheric plasma, plasma diagnosis, emission spectroscopy, gas temperature

1. Introduction

In the last twenty years, the development of non-thermal plasma sources well-controlled and open to the atmosphere, generating *cold atmospheric plasmas* (CAPs) at temperatures under 40 ºC, has proliferated opening new horizons in fields such as biomedicine, food preservation, and agriculture [1-3]. CAPs emerge as a very appealing technology because of their easy handling (they run at atmospheric pressure, so without the restrictions imposed by vacuum systems), their low power consumption, along with their ability to generate active species, in great quantity and diversity. Controlling the gas temperature (T_g) of CAPs is particularly relevant when it comes to applying cold plasma jets directly on living human

(and animal) cells, tissues and organs, and in the treatment of foods and plants.

Since CAP sources run open to the atmosphere, there is an interaction plasma-air, which eventually results in the generation of abundant amounts of reactive oxygen and nitrogen species, also known as ROS and RNS respectively (more generally RONS). Recent studies have shown that RONS play an outstanding role in the biological action of CAPs [4-12]. Thus, knowing all species generated in CAPs is one main step to understand, control, and manage their biological effects.

The development of new diagnosis techniques allowing both the identification of species created in CAPs (and their concentrations) and obtaining reliable values of the gas temperature is of great interest, along with the development of models aiming at understanding the plasma-tissue (food/plant) interaction.

Argon is commonly used in the operation of CAPs reactors because it is a cheap inert gas. Some of these reactors, such as PlasmaDerm, kiNPEn, or MicroPlaSter, have even been marketed as therapeutic tools. As they are generated in the open atmosphere, unknown amounts of air (dependent on the experimental conditions) enter the plasma region. To have an estimation of the proportion of air in these discharges is of paramount importance from the perspective of their modeling. Also, it would help to understand experimental results dealing with the behavior and effectiveness of the different plasma sources determined by the amount and variety of species in them.

The gas temperature in atmospheric-pressure plasmas is frequently determined from UV-Optical Emission Spectroscopy (UV-OES) techniques based on the analysis of molecular emission spectra. Under such a high-pressure condition, translational and rotational energy states are strongly coupled, and the rotational temperature resulting from them is a good estimate of the kinetic temperature of the plasma heavy particles (ions and neutrals). However, the application of molecular emission spectroscopy techniques for gas temperature determination in plasmas is sometimes complex and should be done carefully [13]. Thus, for instance, an overlap of bands or a population distribution of rotational levels with a non-Boltzmann nature prevents getting reliable values of gas temperature. Besides, some of these techniques are not sensitive to variations of the gas temperature near the room temperature (so, under CAP conditions) [14].

More recently, they have been developed alternative OES methods allowing the gas temperature determination in non-thermal plasmas, based on the analysis of profiles of some specific atomic lines. The main feature of these methods is they do not rely on thermodynamic equilibrium assumptions. Christova and colleagues proposed, for the first time, the use of the *van der Waals* broadening of some argon atomic lines for the determination of the plasma gas temperature [15]. Briefly, this technique, further developed in [16,17], consists in the measurement of argon atomic lines not experiencing resonance broadening (also dependent on T_g), namely Ar I 425.94, 522.13, 549.61 and 603.21 nm. Because, these lines have a non-negligible *Stark* broadening (dependent on electron density) for electron densities above 10^{14} cm^{-3}, this technique requires previous determination of this plasma parameter. Yubero and colleagues proposed an approach using pairs of these lines in order to bypass this dependence on the electron density [18].

Pipa and colleagues [14] developed a method based on the measurement of the *resonance* broadening Ar I 750.39, 826.45, 840.82, 852.14, 922.45, and 978.45 nm emission lines. These lines correspond to transitions into the resonance level s_2 of the $3p^5 4s$ configuration. For electron densities lower than 10^{15} cm^{-3}, these lines have a negligible Stark broadening. They also considered negligible the van der Waals broadening of these lines.

More recently, we analysed in detail the relative importance of resonance and van der Waals broadenings of all argon atomic lines corresponding to transitions into resonance levels *s2* and *s4* of the *3p54s* configuration [19]. In that work, we demonstrated for these lines the van der Waals contribution to the entire broadening should be considered under any gas temperature condition. We also proposed new methods to measure the gas temperature in pure argon plasmas from the collisional broadening of any of these lines. When these methods were applied to a plasma jet, results from them showed some discrepancies for plasma positions in contact with air, which were minimized considering a typical proportion of air in calculations.

On the basis that van der Waals and resonance contributions depend on the composition of the gas supporting the discharge, in a specific way for each of the argon lines in reference [19] (as it will be shown in next section), in the present work we propose a new approach based on the use of two of these lines, enabling simultaneous determination of gas temperature and amount of air in non-thermal argon plasma jets with gas temperatures below 2000 K and electron densities under 10^{15} cm^{-3} (so, including argon CAPs). For non-thermal plasma jets operating in other gases, similar methods using different atomic lines (He I, O I…) could be also developed. In contrast to other OES techniques, this new method has the additional advantage of no relying on thermodynamic equilibrium assumptions and not being affected by spatial non-uniformities as these broadenings are determined by local particle collisions.

The method has been applied to the case of an argon microwave-induced plasma jet (2.45 GHz). For validation purposes, a comparison of T_{gas} to the rotational temperature, derived after the N_2 rovibrational band simulations, was done.To the best of the author's knowledge, this is the first

time that OES is being used to evaluate the fraction of air in a plasma.

2. Method

In plasmas generated at atmospheric pressure, the emission of atoms broads due to different effects. For a detailed description of these broadening mechanisms, the reader is referred to references [13,14,17,20].

Briefly, lines emitted by an unmagnetized plasma are generally affected by (i) the *natural broadening*; (ii) the *Doppler broadening*; and (iii) the *collisional broadening*. Emission from the plasma could be partially self-absorbed as it propagates within it. This self-absorption phenomenon artificially modifies the broadening of lines and is difficult to quantify. For this reason, atomic lines non-affected by self-absorption are preferably used for plasma diagnosis. Finally, when lines are detected by the optical system, they also experience an *instrumental broadening*, determined by the dispersion and the width of the slits when a spectrometer is used for the detection of light [20].

Because the *natural broadening* is typically in the order of 0.00001 nm, it is neglected in atmospheric pressure plasma spectroscopy.

The *Doppler broadening* originates a Gaussian-shaped line profile with a full-width at half-maximum (FWHM), W_D, dependent on the line wavelength (λ), the gas temperature in the plasma and the mass of the radiating atoms [20].

The *collisional broadening* encompasses *van der Waals*, *resonance*, and *Stark* broadenings originated by disturbing particles of different nature. The *van der Waals* broadening is due to neutral perturbers and originates line profiles with a Lorentzian shape, whose FWHM (W_W) is determined by T_g and it is also dependent on λ, the nature of the emitter atoms, and the nature of perturbers, all gathered in C_W constant [19]

$$W_W(T_g) = \frac{C_W}{T_g^{0.7}}(\text{nm}) \tag{1}$$

The value of this constant for a specific Ar I line can be calculated using expressions in [19] and taking into account the considerations below. In a pure argon plasma, argon atoms would be the only perturbers surrounding emitters, so reduced mass Ar-Ar ($\mu_{Ar\text{-}Ar}$ = 19.97) and argon polarizability (α_{Ar} = $16.54\cdot10^{-25}$ cm^3) must be used for the determination of C_W^{Ar}. In argon plasmas containing air, air molecules should be also considered as perturbers and in that case, reduced mass Ar-Air ($\mu_{Ar\text{-}Air} \approx 16.81$) and air polarizability ($\alpha_{Air} \approx 2.10\cdot10^{-23}$ cm^3) need be considered to determine C_W^{Air}. In this way, for an argon jet (open to the air), the following expression of the van der Waals broadening would account for the air entrainment into the plasma [13]

$$W_W(T_g, \chi_{Air}) = \chi_{Ar}\frac{C_W^{Ar}}{T_g^{0.7}} + \chi_{Air}\frac{C_W^{Air}}{T_g^{0.7}}(\text{nm}) = \\ = (1-\chi_{Air})\frac{C_W^{Ar}}{T_g^{0.7}} + \chi_{Air}\frac{C_W^{Air}}{T_g^{0.7}}(\text{nm}) \tag{2}$$

being χ_{Ar} and χ_{Air} the molar fractions of argon and air, respectively [17].

On the other hand, dipole-dipole interactions of the emitter with ground-state atoms of the same element are responsible for the *resonance broadening*. This broadening leads to a Lorentzian shaped profile, whose FWHM (W_R) depends again on T_g and λ of the line, in addition to some spectroscopic parameters (oscillator strength, wavelength, the statistical weights of its upper and lower levels) of the so-called *resonance lines* involved in each case [19]. Again, all these dependencies can be gathered in a constant C_R in such a way that W_R can be written as

$$W_R(T_g) = \frac{C_R}{T_g}(nm) \tag{3}$$

Let's remind that this broadening is not affecting every single spectral line in the spectrum, but only those corresponding to transitions with upper and lower levels having electric dipole transitions to the ground state.

When a fraction of air is present in the discharge, the proportion of argon atoms in the ground state reduces, and the expression (3) should be modified as follows

$$W_R(T_g, \chi_{Air}) = \chi_{Ar}\frac{C_R}{T_g}(\text{nm}) = (1-\chi_{Air})\frac{C_R}{T_g}(\text{nm}) \tag{4}$$

The *Stark broadening* of the line is caused by charged particles around the emitter atom. In non-thermal plasmas, electrons are responsible for the foremost part of this broadening (due to their higher velocities compared with that of ions). For argon atoms (non-hydrogenic), the Stark broadening due to electrons results in a profile that can be approximated to a Lorentzian function, and whose FWHM, W_S, depends on the electron density (n_e) and the electron temperature (T_e) (through the so-called Stark parameter $w_e(T_e)$) as follows [21-24]:

$$W_S(T_e, n_e) \approx w_e(T_e)\frac{n_e}{10^{16}} \tag{5}$$

In summary, the collisional broadening (resulting from *van der Waals*, *resonance*, and *Stark* mechanisms) leads to a Lorentzian-shaped profile with an FWHM, W_C, given by:

$$W_C(T_g, \chi_{Air}, n_e, T_e) = W_W(T_g, \chi_{Air}) + W_R(T_g, \chi_{Air}) + W_S(n_e, T_e) \quad (6)$$

Using entrance and exit slits of equal width during detection with the spectrometer, the instrumental function can be approximated to a Gaussian profile with an FWHM, W_I, given by

$$W_I = D(\lambda) l_S \quad (7)$$

where l_s is the slit width and $D(\lambda)$ the dispersion of spectrometer, which depends on wavelength. For each line and given slit widths, this broadening can be determined.

Finally, the detected profile of a no self-absorbed line (resulting from the combination of Doppler, collisional and instrumental broadenings) can be reasonably well fitted in many cases to a Voigt function [15-20], whose FWHM (W_V), is given by:

$$W_V \approx \frac{W_C}{2} + \sqrt{\left(\frac{W_C}{2}\right)^2 + W_D^2 + W_I^2} \quad (8)$$

In this work, we propose a new tool allowing the simultaneous determination of T_g and the fraction of air in the plasma. The method is based on the measurement of the collisional broadening of two (non-self-absorbed) argon atomic lines, namely Ar I 840.86 and Ar I 842.46 nm. These lines correspond to transitions into the resonance levels s_2 and s_4, respectively, of the $3p^5 4s$ configuration, so they have a relatively large resonance broadening (particularly high in the case of the Ar I 840.86 nm line).

In previous work, we have shown that, for electron densities under 10^{15} cm^{-3}, resonance and van der Waals broadenings of both lines are much larger than their respective Stark broadenings [19], so that, the Stark contribution to the total collisional broadening can be neglected. Therefore, under these experimental conditions, W_C of these lines does not vary with n_e and T_e, being only dependent on T_g and χ_{Air}

$$W_C(T_g, \chi_{Air}) \approx W_W(T_g, \chi_{Air}) + W_R(T_g, \chi_{Air}) = (1-\chi_{Air})\frac{C_W^{Ar}}{T_g^{0.7}} + \chi_{Air}\frac{C_W^{Air}}{T_g^{0.7}} + (1-\chi_{Air})\frac{C_R}{T_g}\,(\text{nm}) \quad (9)$$

In this expression, an averaged effect of the air as perturber was considered [19], in the same way as proposed by Laux et al. in [25]. Bruggeman et al. [26] and Garcia et al. [27] did a similar assumption to determine the van der Waals contribution of the line H_β (hydrogen Balmer series) for plasmas in vapor water.

Given that constants C_W^{Ar}, C_W^{Air} and C_R in eq. (9) are characteristics to each specific line, using eq. (9) for two lines (in this case, Ar I 840.86 and Ar I 842.46 nm), T_g and the air fraction in plasma can be determined simultaneously.

Constants C_W^{Ar}, C_W^{Air} and C_R in eq. (9) have been calculated for Ar I 840.86 and Ar I 842.46 nm lines. Data from the NIST atomic database [28] and expressions in [19] were used for this purpose. In this way, the following values were obtained: C_W^{Ar}(Ar I 840.86 nm) = 2.100, C_W^{Air}(Ar I 840.86 nm) = 6.110, C_R(Ar I 840.86 nm) = 67.519, C_W^{Ar}(Ar I 842.46 nm) = 1.891, C_W^{Air}(Ar I 842.46 nm) = 5.502, C_R(Ar I 842.46 nm) = 16.802.

On the other hand, because of the Doppler broadening of the lines Ar I 840.86 and Ar I 842.46 nm only becomes important for values of gas temperature higher than 2000 K [19], eq. (8) can be written for plasmas with T_g < 2000 K as follows

$$W_V \approx \frac{W_C}{2} + \sqrt{\left(\frac{W_C}{2}\right)^2 + W_I^2} \quad (10)$$

Therefore, the whole procedure would be the following. Firstly, W_V would be obtained from the experimentally measured profile, by fitting it to Voigt shaped profile. Subsequently, knowing W_I, the collisional broadening would be derived from

$$W_C = W_V - \frac{W_I^2}{W_V} \quad (11)$$

Finally, using eq. (9) for Ar I 840.86 and Ar I 842.46 nm, unknowns T_g and χ_{Air} could be obtained.

As solving this system of equations is not straightforward, this technique has been simplified through the graphical method shown in Figure 1. This figure plots theoretical W_C (Ar I 842.46 nm) versus theoretical W_C (Ar I 840.86 nm) for different T_g and air molar fractions. It also includes a calculation example corresponding to a case in which W_C (Ar I 840.86) and W_C (Ar I 842.46) measured were 0.0808 and 0.0385 nm, respectively. In this example, the gas temperature and air fraction obtained were 900 K and 30%, respectively.

Let's remark that, as shown in Figure 1, the method becomes progressively more accurate as the gas temperature reduces and (in less extent) as the fraction of air does, so it is particularly adequate for CAPs.

Although in this work, the method has been developed for lines Ar I 840.86 and Ar I 842.46 nm (they are two of the most intense atomic argon lines and are isolated in the spectrum not

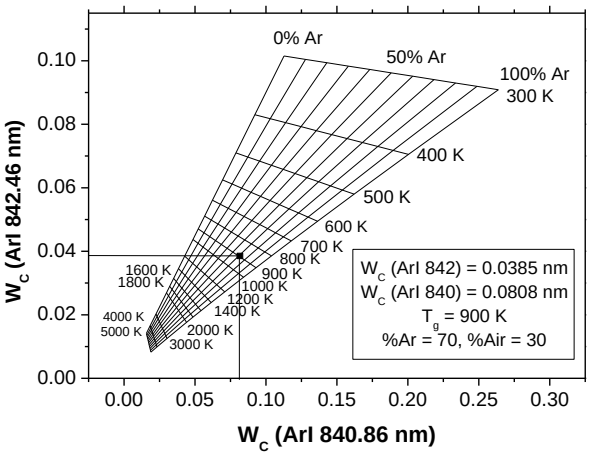

Figure 1. Theoretical dependence of W_C (Ar I 842.46 nm) and W_C (Ar I 840.86 nm) on T_g and air molar fractions.

overlapping with other peaks), other pairs of lines could be used as long as they fulfill the following conditions: (i) having a Stark broadening with a negligible contribution to the full collisional broadening (so a small value in comparison to resonance + van der Waals broadenings), (ii) undergoing negligible self-absorption and (iii) having broadenings with very different dependence on gas temperature and air amount, i.e. different C_R and C_W coefficients in Eq. 13. Pairs of argon lines corresponding to transitions into the resonance levels s_2 and s_4 of the $3p^5 4s$ configuration, respectively, satisfy these conditions.

3. Measuring the gas temperature and the air proportion in a microwave sustained plasma jet

3.1 Experimental set-up

The microwave (2.45 GHz) plasma jet was generated with the help of a *surfatron* [29] (see Figure 2) inside a quartz tube (of 1.5 and 4 mm of inner and outer diameter, respectively) opened to the air. This device launched azimuthally symmetric surface-waves, which mainly propagate through the dielectric-plasma interface, thus sustaining the plasma column inside the dielectric tube. In this way, microwave powers ranging from 30 to 200 W were coupled to the support gas (argon with a purity of ≥ 99.99 %). A calibrated mass flow controller was used for argon flow-rate adjustment at 0.5, 1.0 and 1.5 L/min. Figure 2 also schematizes the experimental acquisition system of UV-OES measurements. Light emission from the plasma axial position y = 18 mm (measuring y from the surfatron) was analyzed by using a 1 m focal length spectrometer (Jobin-Yvon THR1000, Czerny-Turner type), equipped with a 1200 grooves/mm holographic grating. A R636 Hamamatsu photomultiplier was used as a detector. The light from the plasma was transversely collected and focussed onto an optical fiber using an achromatic lens.

The instrumental function of the spectrometer for these wavelengths was measured following the procedure explained in reference [19]. For a 37 μm slit width, W_I (Ar I 840.82 nm) = 0.02827 nm and W_I (Ar I 842.46 nm) = 0.02829 nm.

On the other hand, in the chosen direction of observation (side-on), this plasma (of 1.5 mm max. diameter) can be considered optically thin for the lines Ar I 840.82 nm and 842.46 nm used in this work, as shown by Garcia *et al.* [30]. From light absorption measurements using an intense calibrated lamp, these authors measured a scape factor $\Lambda = 1$. In that study, lines with self-absorption were also identified because their populations deviated from the obtained Atomic State Distribution Function. Thus, lines Ar I 840.82 nm and 842.46 nm did not suffer self-absorption.

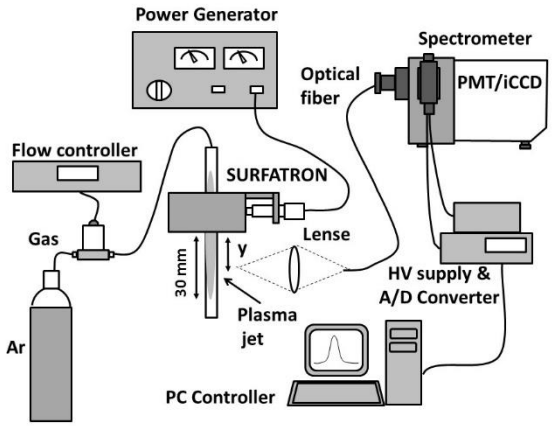

Figure 2. Experimental set-up.

In order to validate the gas temperature values measured, this magnitude was also estimated from the rotational temperature of the N_2 (C-B) rovibrational band (2^{nd} positive system). For this purpose, its emission at the region 350-360 nm was recorded and MassiveOES code developed by Voráč et al. [31] was used for the simulation the band at different rotational and vibrational temperatures. From the fitting of the simulated band to experimentally measured spectrum, the gas (rotational) temperature was estimated. Figure 3 illustrates an example of this fitting (for P = 150 W and F = 1 L/min).

Additionally, H I 486.13 nm line (Balmer series, H_β) was also recorded. Values of electron density derived from this line following the procedure described in [20], were lower than 10^{15} cm^{-3} (ranged between 1.4 and $4 \cdot 10^{14}$ cm^{-3}). So, based on previously explained considerations, the Stark mechanism broadening could be neglected.

The axial evolution of the emission of some atomic lines was also recorded. For this purpose, an iCCD (LAVISION Flamestar4) was used.

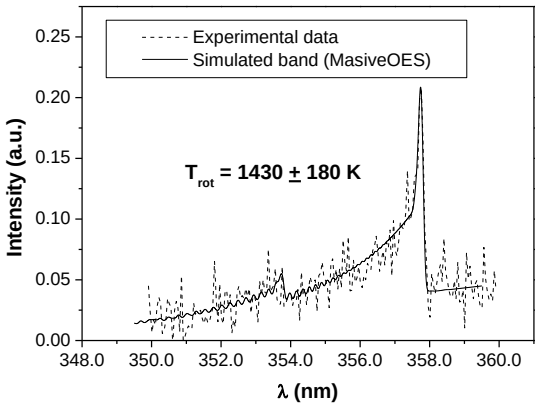

Figure 3. Fitting of experimenal N_2 rovibrational data to simulated N_2 rovibrational band by MasiveOES.

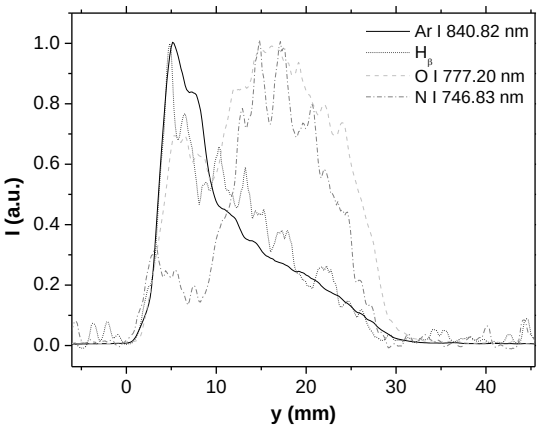

Figure 5. Axial changes for the intensities of the lines Ar I 840.82 nm, H_β, O I 777.20 nm, and N I 746.83 nm along the plasma jet (P = 150, F = 1 L/min).

3.2 Results

Figure 4 shows a typical emission spectrum recorded for this microwave plasma jet (P = 150 W, F = 1 L/min). The presence of N_2 bands and oxygen and nitrogen atomic lines reveals the air was indeed entering into the plasma. Axial changes for the intensities of the lines Ar I 840.82 nm, H_β, O I 777.20 nm, and N I 746.83 nm along the plasma jet in Figure 5 show that main excitation for nitrogen and oxygen atoms took place at positions closer the end of this plasma column with a maximum at $y \sim 18$ mm (when P = 150 W, F = 1 L/min). This indicates these species are reaching the plasma through the end of the tube. For this reason, measurements of air fraction and gas temperature were done at y = 18 mm. On the contrary, the highest excitation of argon and hydrogen (coming from the gas bottle) takes place at the positions next to the surfatron. For the rest of experimental conditions, measurents were also performed at this axial position.

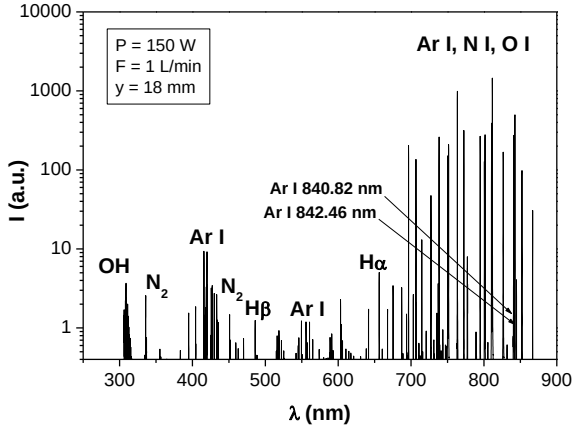

Figure 4. Characteristic emission spectrum emitted by the microwave argon plasma jet (P = 150 W, F = 1 L/min).

Table 1 gathers the collisional broadenings of the lines Ar I 840.82 nm and Ar I 842.46 nm emitted by the microwave plasma jet and measured under different operating conditions. From these values and using eq. (9) (or the plot in Figure 1), gas temperature and air fraction were obtained. Figure 6 shows the graphical determination of these parameters from the theoretical surface. Table 2 gathers results from it.

Table 1. Collisional broadening of Ar I 840.82 mn and Ar I 842.46 nm lines in a microvawe-sustained argon plasma jet running at different experimental conditions.

F_{Ar} (slm)	P(W)	$W_{C,\,840}$(nm)	$W_{C,\,842}$(nm)
0.5	30	0.0756 ± 0.0004	0.0325 ± 0.0004
	75	0.0632 ± 0.0004	0.0283 ± 0.0004
	150	0.0561 ± 0.0004	0.0262 ± 0.0003
	200	0.0507 ± 0.0005	0.0238 ± 0.0006
1.0	30	0.0816 ± 0.0004	0.0358 ± 0.0004
	75	0.0680 ± 0.0004	0.0307 ± 0.0004
	150	0.0556 ± 0.0006	0.0242 ± 0.0005
	200	0.0588 ± 0.0004	0.0276 ± 0.0003
1.5	30	0.0823 ± 0.0003	0.0380 ± 0.0004
	75	0.0703 ± 0.0003	0.0317 ± 0.0003
	150	0.0647 ± 0.0003	0.0321 ± 0.007
	200	0.0617 ± 0.0004	0.0290 ± 0.0003

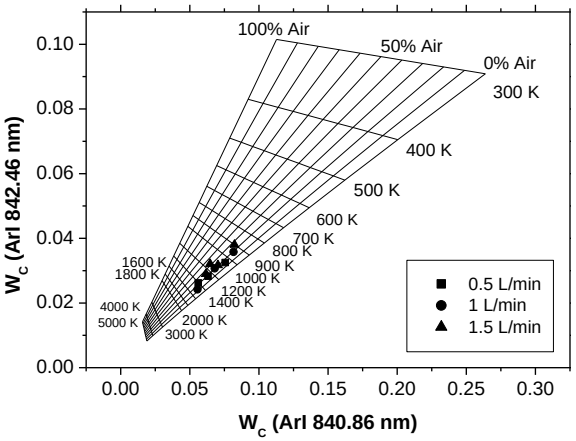

Figure 6. Graphical determination of gas temperature and air fraction in a microwave argon plasma jet under different experimental conditions.

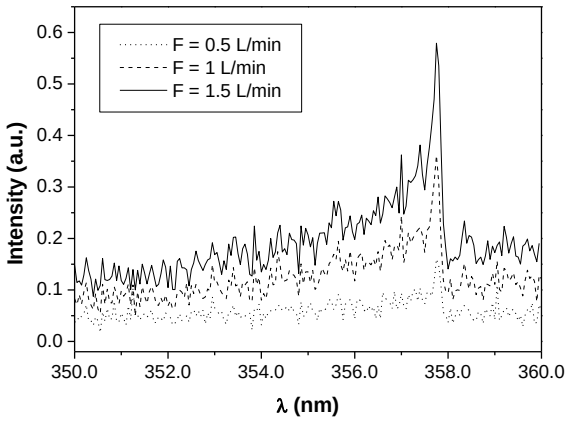

Figure 7. N_2 rovibrational bands measured at different gas flow-rates (P = 150 W, y = 18 mm).

Table 2. Gas temperature and air fraction in a microvawe argon plasma jet running at different experimental conditions.

F_{Ar} (L/min)	*P*(W)	T_g(K)	*% air*
0.5	30	1050 ± 30	15 ± 3
	75	1260 ± 30	18 ± 4
	150	1410 ± 20	22 ± 2
	200	1530 ± 40	13 ± 5
1.0	30	945 ± 15	19 ± 2
	75	1150 ± 20	20 ± 3
	150	1490 ± 40	12 ± 5
	200	1332 ± 15	23 ± 2
1.5	30	900 ± 10	26 ± 3
	75	1100 ± 10	19 ± 2
	150	1170 ± 40	28 ± 3
	200	1257 ± 15	24 ± 2

In general, in this plasma jet, the gas temperature grows when the power increases, under all flow rate conditions. On the contrary, the higher the flow rate, the lower the gas temperature. These results agree with others found in previous work [30].

The fraction of air in the plasma ranged between 12 ± 5 and 28 ± 3 %. For a fixed argon flow rate, this parameter has rather constant values, within the error range. Its mean values were 17%, 18.5%, and 24.5% for 0.5, 1.0 and 1.5 L/min, respectively. Thus, bigger amounts of air seem to be reaching the plasma at progressively higher argon flow rates. This increase is consistent with the rise in the emission of species coming from air observed at high flow-rates, and it is likely produced by the effect of turbulences at the exit of the tube under this high flow conditions. Figure 7 shows an example of this rise for N_2 (C) species at y = 18 mm.

The errors of the method in this plasma jet with gas temperatures above 1000 K are bigger than those expected for CAPs at temperatures under 320 K. A bigger plot of Figure 1, has been included as supplementary information as Figure S1, to be used by the reader.

On the other hand, Table 3 shows the values of gas temperature measured from the simulation of the N_2 band at the region 350-360 nm using MassiveOES. A good agreement was found.

Table 3. Gas temperature derived simulation of N_2 band at the region 350-360 nm.

F_{Ar} (L/min)	*P*(W)	$T_{g,\,N2}$ *(K)*
0.5	30	undetectable
	75	1160 ± 210
	150	1260 ± 190
	200	1410 ± 230
1.0	30	980 ± 240
	75	1130 ± 240
	150	1430 ± 180
	200	1400 ± 200
1.5	30	1100 ± 400
	75	1180 ± 160
	150	1130 ± 150
	200	1250 ± 140

4. Final remarks

In this work, we present a new spectroscopic method allowing the simultaneous determination of the gas temperature and air fraction in argon plasma jets in contact with air. It applies to non-thermal argon jets with gas temperatures under 2000 K and electron densities bellow 10^{15} cm^{-3}, which includes CAPs (as commercialized PlasmaDerm or kiNPEn). Nonetheless, the method could be properly modified to be applied to CAPs (or more gereally, to non-thermal plasmas with gas temperatures below 2000 K) operating with other noble gases as Helium.

In addition to having the interesting advantages related to OES techniques (easy to implement and not altering plasma properties), this method also provides the benefits of being very sensitive at low gas temperatures and no-based on thermodynamic equilibrium assumptions.

The new OES method proposed in this work was applied to an argon microwave jet open to the air. Values of the gas temperatures obtained from it were compared to the rotational temperatures derived from the N_2 rovibrational band and a very good agreement was found.

Acknowledgments

The authors thank the MINECO (project MAT2016-79866-R) for financial support.

References

[1] Woedtke T, Reuter S, Masur K, and Weltmann KD 2013 *Physics Reports* **530** 291
[2] Randeniya LK and Groot GJJB 2015 *Plasma Proces Polym* **12** 608
[3] Dasan BG, Onal-Ulusoy B, Pawlat J, Diatczyk J, Sen Y, and Mutlu M 2017 *Food Bioprocess Technol* **10** 650
[4] Graves DB 2012 *J Phys D: Appl Phys* **45** 263001
[5] Ahn HJ 2011 *PLoS ONE* **6** e28154
[6] Kaneko T, Sasaki S, Takashima K, and Kanzaki M 2017 *J Clin Biochem Nutr* **60** 3
[7] Tanaka H, Nakamura K, Mizuno M, Ishikawa K, Takeda K, Kajiyama H, Utsumi F, Kikkawa F, and Hori M 2016 *Scientific Reports* **6** 36282
[8] Canal C, Fontelo R, Hamouda I., Guillem-Marti J, Cvelbar U, and Ginebra MP 2017 *Free Radical Biology and Medicine* **110** 72
[9] Gümbel D, Bekeschus S, Gelbrich N, Napp M, Ekkernkamp A, Kramer A, and Stope MB 2017 *Int J Mol Sci* **18** 2004
[10] Liu Y, Tan S, Zhang H, Kong X, Ding L, Shen J, Lan Y, Cheng C, Zhu T, and Xia W 2017 *Scientific Reports* **7** 7980
[11] Sato Y, Yamada S, Takeda S, Hattori N, Nakamura K, Tanaka H, Mizuno M, Hori M, and Kodera Y 2018 *Ann Surg Oncol* **25** 299
[12] Szili EJ et al. 2018 *Plasma Sources Sci Technol* **27** 014001
[13] Yubero C, García MC, Varo M, and Martínez P 2013 *Spectrochimica Acta B* **90** 61
[14] Pipa AV, Ionikh Y, Chekishev VM, Dünnbier M and Reuter S 2015 *Appl Phys Lett* **106** 244104
[15] Christova M, Castaños-Martinez E, Calzada MD, Kabouzi Y, Luque JM, and Moisan M 2004 *Appl Spectrosc* **58** 1032
[16] Christova M, Gagov V and Koleva I 2000 *Spectrochim Acta B* **55** 815
[17] Yubero C, Dimitrijevic MS, García MC and Calzada MD 2007 *Spectrochim Acta B* **62** 169
[18] Yubero C, Rodero A, Dimitrijevic MS, Gamero A and García MC 2017 *Spectrochim Acta B* **129** 14
[19] Rodero A and García MC 2017 *J Quant Spectrosc & Radiat Transfer* **198** 93
[20] Nikiforov AY, Leys C, Gonzalez MA, Walsh JL 2015 *Plasma Sources Sci Technol* **24** 034001
[21] Konjevic N 1999 *Phys Rep* **316** 339
[22] Konjevic N and Wiese WL 1990 *J Phys Chem Ref Data* **19** 1307
[23] Konjevic N, Lesage A, Fuhr JR, and Wiese WL 2002 *J Phys Chem Ref Data* **31** 819
[24] Griem HR 1974 *Spectral line broadening by plasmas*, New York: Academic Press
[25] Laux CO, Spence TG, Kruger CH, and Zare RN 2003 *Plasma Sources Sci Technol* **12** 125
[26] Bruggeman P, Schram D, González MA, Rego R, Kong MG, and Leys C 2009 *Plasma Sources Sci Technol* **18** 025017
[27] García MC, Gucker SN and Foster JE 2015 *J Phys D: Appl Phys* **48** 355203
[28] Kramida A, Ralchenko Y and Reader J 2016 NIST ASD Team, NIST Atomic Spectra Database (version 5.7), available at http://physics.nist.gov/asd [Thu Jan 20, 2020]
[29] Moisan M and Pelletier J 1992 *Microwave excited plasmas* **Chap 3** Elsevier Amsterdam
[30] García MC, Rodero A, Sola A and Gamero A 2000 *Spectrochimica Acta B* **55** 1733
[31] Voráč J, Synek P, Potočňáková L, Hnilica J and Kudrle V 2017 *Plasma Sources Sci Technol* **2** 025010.